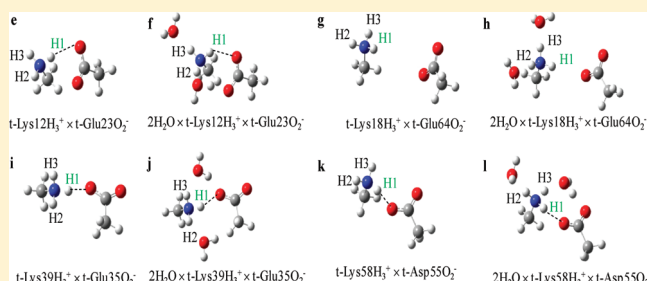


Ab Initio Calculations of Deuterium Isotope Effects on Chemical Shifts of Salt-Bridged Lysines

Saif Ullah,^{*,†} Takayoshi Ishimoto,[‡] Mike P. Williamson,[§] and Poul Erik Hansen[†][†]Department of Science, Systems and Models, Roskilde University, P.O. Box 260, DK-4000 Roskilde, Denmark[‡]INAMORI Frontier Research Center, Kyushu University, 744 Motooka, Nishi-ku, Fukuoka, 819-0395, Japan[§]Department of Molecular Biology and Biotechnology, University of Sheffield, Firth Court, Western Bank, Sheffield, S10 2TN, United Kingdom

ABSTRACT: Deuterium isotope effects measure the change in chemical shift on substitution of a proton by deuterium. They have been calculated by direct treatment of the H/D nuclear quantum effect using a multicomponent ab initio molecular orbital method based on a non-Born–Oppenheimer approximation. This method enables the determination of both the electronic and the protonic (deuteronic) wave functions simultaneously and can directly calculate the geometrical difference induced by H/D isotope effects. The calculations show that the one-bond deuterium isotope effects on ^{15}N nuclear shielding, $^1\Delta^{15}\text{N}(\text{D})$, in ammonium and amines decrease as a counterion or water molecule moves closer to the nitrogen. $^1\Delta^{15}\text{N}(\text{D})$ and $^2\Delta^1\text{H}(\text{D})$ of the NH_3^+ groups of lysine residues in the B1 domain of protein G have been calculated using truncated side chains and also determined experimentally by NMR. Comparisons show that the structures in solution are different from those in the crystal and that solvation plays an important role in weakening the hydrogen bonds.



INTRODUCTION

Hydrogen bonds are important weak noncovalent interactions.^{1,2} An important subclass of hydrogen bonds is salt bridges, which are hydrogen bonds between two charged groups. Proteins have numerous basic (Arg, Lys) and acidic (Asp, Glu) residues which make up about a quarter of the residues on an average protein and can form salt bridges in which the protonated basic side chain ($\text{R}-\text{NH}_3^+$) interacts with a negatively charged acidic side chain ($\text{R}-\text{COO}^-$). Buried salt bridges appear to be important in protein structure and stability,^{3–5} while the role of solvent-exposed salt bridges is more controversial. Experimental investigations of the contribution of solvent-exposed salt bridges to protein stability find them anywhere from stabilizing⁶ to destabilizing⁷ via insignificant interactions.^{5,8–10}

Historically, isotopic substitution has been of great use in probing hydrogen bonding. The deuterium isotope effect on the shielding of nucleus X due to the substitution of X–H by X–D can be obtained¹¹ by using eq 1,

$$^n\Delta X(\text{D}) = \sigma X(\text{D}) - \sigma X(\text{H}) = \delta X(\text{H}) - \delta X(\text{D}) \quad (1)$$

where n is the intervening number of bonds from the deuterium substitution to the nucleus X; $\sigma X(\text{D})$ and $\delta X(\text{D})$ are the absolute shielding and corresponding chemical shift of X. All values discussed in the paper correspond to the effect due to a single deuterium substitution attached to N, and focus on the isotope effects seen on lysine side chains, namely, $^1\Delta^{15}\text{N}(\text{D})$ and $^2\Delta^1\text{H}(\text{D})$.

The simplest model for lysines is the ammonium ion, for which deuterium isotope effects on ^1H and ^{15}N chemical shifts have been studied intensely.^{12–15} The isotope effects showed dependence on counterions and gave by extrapolation to infinite dilution values of 0.26 ppm for $^1\Delta^{15}\text{N}(\text{D})$ and -0.017 ppm for $^2\Delta^1\text{H}(\text{D})$. It was furthermore seen that the influence of hard ions like nitrate, perchlorate, and acetate had effects very similar to water.¹⁵ It was later shown by ab initio calculations that directional counterions (ie, ions making hydrogen bonds directed along or closely aligned to the N–H bond) or molecules such as water or charges are very important for the magnitude of $^1\Delta^{15}\text{N}(\text{D})$ and even for the sign of $^2\Delta^1\text{H}(\text{D})$.^{11,15} It was furthermore demonstrated in cryptands and podands that $^1\Delta^{15}\text{N}(\text{D})$ depends on the $\text{N}\cdots\text{N}$ or $\text{N}\cdots\text{O}$ distance.¹² Solvation of ammonium ions has been investigated in great detail, and directional hydrogen bonding is found to dominate.¹⁶ Deuterium isotope effects on chemical shifts can be used to gauge solvation as well as provide information about the nature and distance to counterions.

Deuterium isotope effects on chemical shift can be calculated as demonstrated by Jameson¹⁷ by calculating the change in nuclear shielding as well as the change in the bond length upon deuteration. The latter has traditionally been done by mapping out the potential energy as a function of bond length.¹⁸ This is

Received: November 23, 2010

Revised: January 23, 2011

clearly a very time-consuming procedure. In addition, although it is one of the important topics to theoretically estimate the hydrogen bond length upon deuteration, the conventional molecular orbital method does not fully describe the explicit geometrical difference upon deuteration. However, attempts to calculate isotope effects more directly are also done.^{19,20} Another direct way to do the latter is to use the multicomponent molecular orbital (MC_MO) method,^{21,22} which is based on the non-Born–Oppenheimer approximation and which has been proposed to be suitable for evaluation of the H/D isotope effect, while some theoretical approaches are recently proposed to describe the hydrogen bonds accurately.^{23,24} The MC_MO method enables us to analyze the quantum effects of a proton (deuteron) in small model molecular systems which directly express geometrical isotope effects including coupling effects between nuclei and electrons.^{25,26} This method also allows fast calculations and non-empirical determinations of isotope effects even in large molecules. In the present study, we have tested this method on simple molecules: ammonium ions and truncated lysines. Four methyl ammonium/acetate pairs corresponding to the truncated side chains of lysines and aspartates or glutamates were chosen as an appropriate model of the lysine–carboxylate salt bridge.²⁷ It is our aim to elucidate theoretically the factors affecting $^1\Delta^{15}\text{N}(\text{D})$ and $^2\Delta^1\text{H}(\text{D})$ in the model methyl ammonium ion to compare with experimental results and to provide a tool to investigate salt bridges in solution especially with respect to heavy atom distances and water solvation.

The salt bridge geometries studied here were obtained from a crystal structure of protein G B1 domain²⁷ in which lysine 12 forms a salt bridge to glutamate 23, lysine 39 to glutamate 35, and lysine 58 to aspartate 55,¹⁰ and they were used in this study because experimental deuterium isotope effects on ^{15}N chemical shifts are available.¹⁰

COMPUTATIONAL DETAILS

Modeling. The structures of lysine and carboxylate ions were cloned from the protein X-ray structure, but only the last carbon of the side chains was included.²⁷ The lysines are therefore referred to as truncated (t-lysine). When we performed the full geometry optimization of t-lysine and carboxylate complex, the proton was transferred from t-lysine to carboxylate group due to the large geometry change in hydrogen bond. This indicates that the full geometry optimization for the hydrogen bonded complex cloned from the protein X-ray structure does not conserve the folded state of the protein. To express the folding structure in protein by the use of t-lysine and carboxylate complex, heavy atom angles, and $\text{RN}\cdots\text{O}$ distances were kept at the experimental X-ray values. All other angles, bond lengths, and hydrogen positions were geometry optimized at the RHF/6-31G(d) level. This model enables to describe the hydrogen bond in a folded structure in the protein. Three water molecules were added around the NH_3^+ group of t-lysine, two water molecules around a truncated lysine-carboxylate complex, and four water molecules around the ammonium ion to treat as explicit hydration water molecules in solvent effect for short range.

H/D Quantum Treatment of MC_MO Calculations. To evaluate the geometrical change induced by H/D isotope substitution, hydrogen bonded protons and deuterons as well as the electrons were treated as quantum waves within the fields of the nuclear point charges by the use of the Hartree–Fock MC_MO (MC_MO-HF) method. A single s-type Gaussian-type function

(GTF), $\exp\{-\alpha(r-R)^2\}$, was employed for each protonic and deuteronic basis function to solve the effective one-particle parameter, f^p , with MO, ϕ_p ,

$$f^p\phi_p = \varepsilon_p\phi_p, f^p = h^p + \sum_p^{N_p} (J_p - K_p) - \sum_i^{N_e} J_i$$

The kinetic energy term, h^p , in one particle operator mainly depends on the nuclear mass. The J and K are Coulomb and exchange operators, respectively. We optimized the center (R) in GTF employed for each protonic and deuteronic basis function to determine the optimum position of proton and deuteron. Values of α of 24.1825 and 35.6214 were used in the protonic and deuteronic GTF, respectively.²² In all calculations using the MC_MO-HF method, the 6-31G(d) basis set was used for the electronic part. One of the problems in using the MC_MO-HF level of theory is the accuracy of the geometrical parameters and of the calculation of the total energy of the H/D systems. For this reason, we calculated the hydrogen bond structure and interaction energy of small $\text{NH}_4^+\cdots\text{H}_2\text{O}$ and $\text{ND}_4^+\cdots\text{H}_2\text{O}$ systems using both MC_MO-HF and second-order Møller–Plesset (MP2) level of MC_MO theory (MC_MO-MP2) methods. The difference in the geometry of the hydrogen bond and interaction energy for H/D systems obtained by MC_MO-HF and MC_MO-MP2 was minimal (within 0.001 Å and 0.01 kcal/mol, respectively). This result indicates that the MC_MO method is sufficiently accurate for quantitative analysis of deuterium isotope effects in our system.

Nuclear Shielding Calculations. The ab initio single point calculations of nuclear shieldings based on the GIAO approach^{28,29} with Gaussian03³⁰ software package at the RHF/6-31G(d) level were performed on the optimized H/D geometries obtained by the MC_MO-HF calculations to analyze one-bond ($^1\Delta^{15}\text{N}$) and two-bond ($^2\Delta^1\text{H}$) deuterium isotope effects on nuclear shieldings.

One bond deuterium isotope effects on ^{15}N chemical shifts, $^1\Delta^{15}\text{N}(\text{D})$, can be calculated using the Jameson formula:¹⁷

$$\begin{aligned} \langle\sigma\rangle - \langle\sigma^*\rangle &= \sum_i \left(\frac{\partial\sigma}{\partial r_i} \right)_e [\langle\Delta r_i\rangle - \langle\Delta r_i\rangle^*] \\ &+ \sum_{ij} \left(\frac{\partial^2\sigma}{\partial r_i\partial r_j} \right)_e [\langle\Delta r_i\Delta r_j\rangle - \langle\Delta r_i\Delta r_j\rangle^*] \\ &+ \sum_{ij} \left(\frac{\partial\sigma}{\partial\alpha_{ij}} \right) [\langle\Delta\alpha_{ij}\rangle - \langle\Delta\alpha_{ij}\rangle^*] + \dots \end{aligned}$$

where deuterated and protonated nitrogen are designated by asterisked and non-asterisked values. This requires calculation of the change in the nuclear shielding at the equilibrium geometry and the change in the NH distance upon deuteration.

RESULTS AND DISCUSSION

MC_MO Calculations for H/D Isotope Effects. The MC_MO-HF calculations were carried out on ammonium ions and on lysines truncated at the final side chain carbon (i.e., methyl ammonium, designated here as t-lysine), as the isolated ions and also hydrated. The optimized geometries of the free NH_4^+ ion, $\text{NH}_4^+\cdots(\text{H}_2\text{O})_4$, side chain non-hydrated t-lysine, and hydrated t-lysine with three water molecules are shown in Figure 1, while the geometries of the hydrogen-bonded lysines

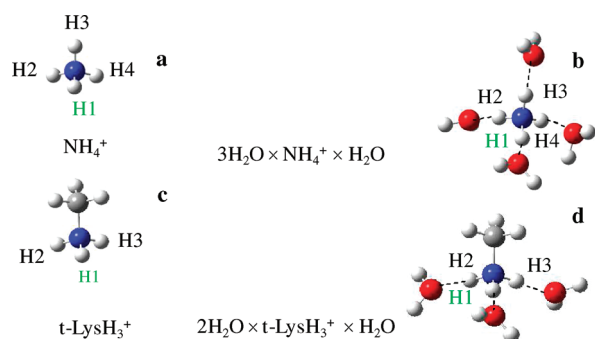


Figure 1. Optimized (MC_{MO}-HF) molecular structures of the non-hydrated ammonium ion (a), 4-fold hydrated ammonium ion (b), non-hydrated truncated lysine (c), and 3-fold hydrated truncated lysine (d). The deuterated hydrogen is marked with a green color.

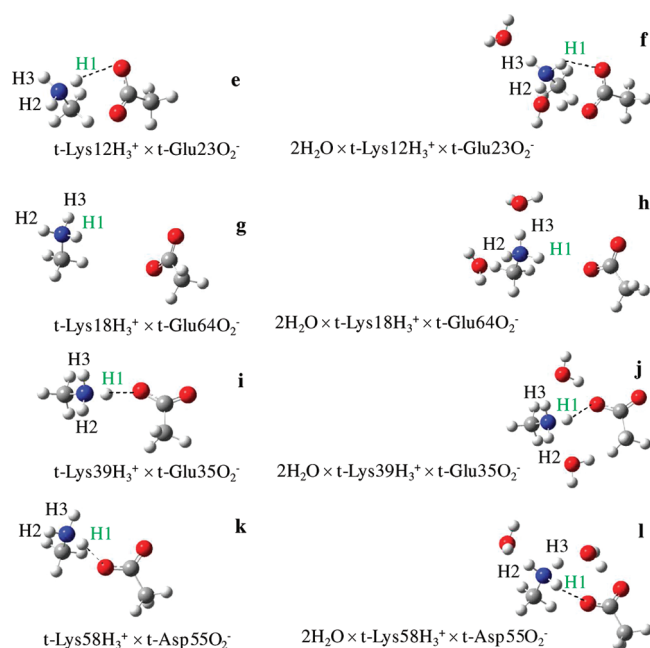


Figure 2. Optimized (MC_{MO}-HF) salt bridge structures of the non-hydrated t-Lys12 complex (e), 2-fold hydrated t-Lys12 complex (f), non-hydrated t-Lys18 complex (g), 2-fold hydrated t-Lys18 complex (h), non-hydrated t-Lys39 complex (i), 2-fold hydrated t-Lys39 complex (j), non-hydrated t-Lys58 complex (k), and 2-fold hydrated t-Lys58 complex (l) from protein G B1 domain. In structures (g) and (h), no hydrogen bond is drawn from NH_3^+ to carboxylate because the distance is too large for hydrogen-bond formation. The deuterated hydrogen is marked with a green color.

in protein G B1 domain and HoxD9 homeodomain are shown in Figures 2 and 3, respectively. For these lysines, the heavy atom locations were kept identical to those in the crystal structures, but hydrogen locations were optimized. The GB1 lysines 12, 18, 39, and 58 are hydrogen bonded to carboxylates on residues 23, 64 (too long for a strong interaction), 35, and 55, respectively (Figure 2), while HoxD9 lysine 57 is hydrogen bonded to a phosphate (Figure 3). To describe the hydrogen bonded systems we use a nomenclature for example $3\text{H}_2\text{O} \times \text{NH}_4^+ \times \text{H}_2\text{O}$ or $2\text{H}_2\text{O} \times \text{t-Lys12H1}^+ \times \text{t-Glu23O}_2^-$ in which it is the H to the left of the second '×' that is deuterated and the molecule on the right is the hydrogen bond partner (or none in case of no hydrogen bonding), whereas the molecules to the left of the first × are the

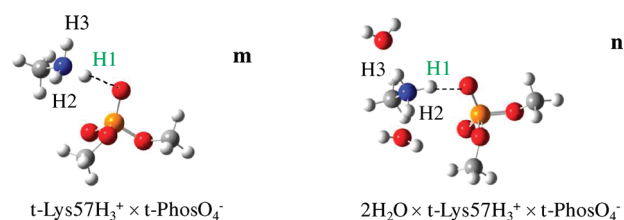


Figure 3. Optimized (MC_{MO}-HF) salt bridge structures of non-hydrated t-Lys57 complex (m) and 2-fold hydrated t-Lys57 complex (n) from the HoxD9 homeodomain. The deuterated hydrogen is marked with a green color.

hydrogen-bond partners to the nondeuterated hydrogens (see Figures 1–3). The MC_{MO} method was used to directly analyze the geometrical difference induced by the H/D quantum effect. The single point nuclear shielding calculations were performed on the optimized geometries obtained by MC_{MO}-HF using the GIAO approach^{28,29} for all of the ionic complexes. Calculated results for ^{15}N and ^1H nuclear shieldings are listed in Table 1.

Optimized N–H(D) distances together with interaction energies are shown in Table 2. The covalent N–D distance is shorter than N–H in all systems due to the anharmonicity of the potential. This result indicates the MC_{MO} method enables us to describe the explicit geometrical difference upon deuteration by the non-empirical procedure. The N–H and N–D distances obtained by optimization of non-hydrated and hydrated ionic species are consistently shorter for the hydrated species. The calculated N–H bond lengths of hydrated ammonium ion and hydrated truncated lysine are 1.039 Å and 1.041 Å, respectively. For the case of hydrated t-Lys18, we obtained two different values of N–H bond lengths (1.041 and 1.049 Å) which are hydrogen-bonded to two water molecules. The proton which is pointing toward the carboxylate group has a shorter N–H bond length (1.03 Å) and has no counterion influence because the acceptor carboxylate group is at a distance of 5.41 Å from the nitrogen atom of the truncated lysine and is therefore too distant to make a significant interaction. Limbach et al. obtained similar N–H bond length values for methylammonium ion surrounded by two and three water molecules optimized at the B3LYP/6-31G(d,p) level.³¹

The values of the interaction energies shown in Table 2 support these conclusions. The difference of interaction energy increases with decreasing N···O distance and becomes smaller upon hydration. However, for the deuterated species the interaction energies are slightly different depending on the position of the deuteration relative to the O^- . When D is pointing toward O^- , it is called a primary isotope effect on interaction energy. When D is not, it is called a secondary isotope effect. Because of the elongation of the hydrogen bond by deuteration (i.e., deuterium exhibits weaker hydrogen bonding than hydrogen), for example the primary interaction energy of the deuterated $\text{t-Lys12H1}^+ \times \text{t-Glu23O}_2^-$ system is 0.56 kcal/mol smaller than that of the protio one. We have clearly demonstrated that the geometrical difference between N–H and N–D reflects to the interaction energy in the hydrogen bond. When the non-hydrogen bonded and hydrated-hydrogen bonded protons, H2 and H3 in Figures 1–3, are replaced by deuterons, the interaction energy between t-lysine and carboxylate group slightly changes (for example, 0.004 and −0.104 kcal/mol for $\text{t-Glu23O}_2^- \times \text{t-Lys12H2}^+$ and $\text{t-Glu23O}_2^- \times \text{t-Lys12H3}^+$, respectively). We also reported primary isotope effects as well as secondary isotope

Table 1. Experimentally and Calculated (GIAO Approach) Deuterium Isotope Effects on ^{15}N and ^1H Nuclear Shieldings in ppm and Heavy Atom Distances in Å^a

system	$\sigma[\text{NH}]$	$\sigma[\text{ND}]$	$^1\Delta^{15}\text{N}$	$^1\Delta^{15}\text{N}_{\text{avg}}^b$	$^1\Delta^{15}\text{N}_{\text{exp}}^c$	$^2\Delta^1\text{H}$	$^2\Delta^1\text{H}_{\text{avg}}^b$	$^2\Delta^1\text{H}_{\text{exp}}^c$	$\text{R}[\text{N}\cdots\text{O}]$
NH_4^+	247.86	248.34	0.48	0.48		0.003	0.003		n.a. ^f
$3\text{H}_2\text{O} \times \text{NH}_4^+ \times \text{H}_2\text{O}$	248.67	249.07	0.41	0.41	0.30 ^g	−0.005	−0.005	−0.018	2.80
t-LysH ⁺	245.21	245.85	0.63	0.63		0.008	0.008		n.a. ^f
$2\text{H}_2\text{O} \times \text{t-LysH}^+ \times \text{H}_2\text{O}$	252.80	253.28	0.48	0.48		−0.016	−0.016		2.82
t-Lys12H1 ⁺ × t-Glu23O ^{−d}	245.06	245.70	0.65			0.003			3.39
t-Glu23O [−] × t-Lys12H2 ⁺ ^d	245.06	245.76	0.70	0.70		0.029	0.021		n.a. ^f
t-Glu23O [−] × t-Lys12H3 ⁺ ^d	245.06	245.82	0.76			0.032			n.a. ^f
$(2\text{H}_2\text{O}) \times \text{t-Lys12H}^+ \times \text{t-Glu23O}^{−e}$	245.96	246.52	0.56			−0.035			3.39
t-Glu23O [−] × t-Lys12H2 ⁺ × $(2\text{H}_2\text{O})^e$	245.96	246.39	0.43	0.45	0.36	−0.031	−0.032	−0.027	2.60
t-Glu23O [−] × t-Lys12H3 ⁺ × $(2\text{H}_2\text{O})^e$	245.96	246.32	0.36			−0.030			2.88
t-Lys18H1 ⁺ × t-Glu64O ^{−d}	244.37	244.99	0.62			0.005			5.41
t-Glu64O [−] × t-Lys18H2 ⁺ ^d	244.37	244.99	0.62	0.63		0.005	0.004		n.a. ^f
t-Glu64O [−] × t-Lys18H3 ⁺ ^d	244.37	245.02	0.64			0.003			n.a. ^f
$(2\text{H}_2\text{O}) \times \text{t-Lys18H}^+ \times \text{t-Glu64O}^{−e}$	247.75	248.47	0.72			0.000			5.41
t-Glu64O [−] × t-Lys18H2 ⁺ × $(2\text{H}_2\text{O})^e$	247.75	248.27	0.52	0.61	0.36	−0.006	−0.002	−0.027	2.80
t-Glu64O [−] × t-Lys18H3 ⁺ × $(2\text{H}_2\text{O})^e$	247.75	248.34	0.58			−0.001			2.88
t-Lys39H1 ⁺ × t-Glu35O ^{−d}	243.93	244.49	0.56			−0.022			3.03
t-Glu35O [−] × t-Lys39H2 ⁺ ^d	243.93	244.65	0.73	0.67		0.011	0.001		n.a. ^f
t-Glu35O [−] × t-Lys39H3 ⁺ ^d	243.93	244.65	0.72			0.013			n.a. ^f
$(2\text{H}_2\text{O}) \times \text{t-Lys39H}^+ \times \text{t-Glu35O}^{−e}$	240.49	241.12	0.63			−0.015			3.03
t-Glu35O [−] × t-Lys39H2 ⁺ × $(2\text{H}_2\text{O})^e$	240.49	241.02	0.53	0.58	0.36	−0.008	−0.012	−0.027	2.78
t-Glu35O [−] × t-Lys39H3 ⁺ × $(2\text{H}_2\text{O})^e$	240.49	241.06	0.57			−0.012			2.65
t-Lys58H1 ⁺ × t-Asp55O ^{−d}	243.69	244.20	0.51			−0.027			2.96
t-Asp55O [−] × t-Lys58H2 ⁺ ^d	243.69	244.42	0.73	0.65		0.007	−0.003	−0.027	n.a. ^f
t-Asp55O [−] × t-Lys58H3 ⁺ ^d	243.69	244.40	0.70			0.010			n.a.
$(\text{H}_2\text{O}) \times \text{t-Lys58H}^+ \times \text{t-Asp55O}^{−e}$	244.83	245.41	0.58			−0.030			2.96
t-Asp55O [−] × t-Lys58H2 ⁺ × $(\text{H}_2\text{O})^e$	244.83	245.29	0.46	0.59		−0.019	0.015		2.90
t-Asp55O [−] × t-Lys58H3 ⁺ × $(\text{H}_2\text{O})^e$	244.83	245.56	0.72			0.004			n.a. ^f
$(2\text{H}_2\text{O}) \times \text{t-Lys58H}^+ \times \text{t-Asp55O}^{−e}$	246.12	246.76	0.64			−0.018			2.96
t-Asp55O [−] × t-Lys58H2 ⁺ × $(2\text{H}_2\text{O})^e$	246.12	246.60	0.48	0.52	0.36	−0.008	−0.018		2.89
t-Asp55O [−] × t-Lys58H3 ⁺ × $(2\text{H}_2\text{O})^e$	246.12	246.55	0.43			−0.028			2.64
t-Lys57H1 ⁺ × t-PhosO ₄ ^{−d}	237.32	237.77	0.44			−0.031			2.86
t-PhosO ₄ [−] × t-Lys57H2 ⁺ ^d	237.32	238.06	0.74	0.63		0.001	−0.009		
t-PhosO ₄ [−] × t-Lys57H3 ⁺ ^d	237.32	238.04	0.72			0.003			
$(2\text{H}_2\text{O}) \times \text{t-Lys57H}^+ \times \text{t-PhosO}_4^{−e}$	245.70	246.17	0.48			−0.029			2.86
t-PhosO ₄ [−] × t-Lys57H2 ⁺ × $(2\text{H}_2\text{O})^e$	245.70	246.13	0.43	0.49	0.35 ^h	−0.024	−0.022		2.65
t-PhosO ₄ [−] × t-Lys57H3 ⁺ × $(2\text{H}_2\text{O})^e$	245.70	246.27	0.57			−0.014			2.88

^a t-Lys12, 18, 39, and 58 refer to protein G²⁷ and t-Lys57 to the HoxD9 homeodomain.³² For structures see Figures 1–3. ^b The calculated figures are the means of relevant individual values; as the hydrogen bonds have similar strengths, deuterium fractionation is not going to play a role, and a geometric mean of the calculated values can be used. ^c Experimentally observed deuterium isotope effects on ^1H and ^{15}N chemical shifts. ^d H1 points toward the carboxylate, while H2 and H3 do not. ^e Hydrated t-lysine: H1 points toward the carboxylate, while H2 and H3 points toward water. ^f No acceptor atom. ^g A similar value is obtained by extrapolation to pure water in ref 12. ^h Taken from ref 32.

effects on interaction energies in different hydrated and non-hydrated complexes (see Table 2).

Analysis of Results. For deuteration at the hydrogen pointing towards the carboxylate anion the isotope effect depends on the $\text{N}\cdots\text{O}$ distance (Figure 4) with a decrease in $^1\Delta^{15}\text{N}(\text{D})$ as the $\text{N}\cdots\text{O}$ distance is decreased. This is similar to what has been found earlier for ammonium ions¹¹ and can be explained as arising from the stronger hydrogen bond removing more electron density from the nitrogen and therefore generating a smaller change in shielding on replacement of H by D.

The two-bond deuterium isotope effects on ^1H , $^2\Delta^1\text{H}(\text{D})$, are also seen to decrease with a decrease in heavy atom $\text{N}\cdots\text{O}$ distances, in accord with $^1\Delta^{15}\text{N}(\text{D})$. A sign inversion of $^2\Delta^1\text{H}(\text{D})$ is observed when deuterium is opposite to water at a short $\text{N}\cdots\text{O}$ distance as previously reported¹¹ (Table 1).

Figure 5 shows the calculated $^1\Delta^{15}\text{N}(\text{D})$ values as a function of the $\text{N}-\text{H}$ distance for ammonium ion, t-Lys, and the salt-bridged t-Lys12, 18, 39, 58 and ethylammonium–carboxylate complex. For the non-hydrated t-lysine series (squares), there is a monotonic decrease in $^1\Delta^{15}\text{N}(\text{D})$ value with the increase in

Table 2. Optimized Hydrogen Bond Distances (Å), Their Differences (H/D), and Interaction Energy and Their Differences (kcal/mol) by MC_MO-HF Calculations^a

system	$r[\text{N}-\text{H}]$	$r[\text{N}-\text{D}]$	Δr	$E_{\text{int}}[\text{H}]$	$E_{\text{int}}[\text{D}]$	ΔE_{int}^b	ΔE_{int}^c
NH_4^+	1.0368	1.0299	−0.0070	n.a.	n.a. ^f	n.a.	n.a.
$3\text{H}_2\text{O} \times \text{NH}_4^+ \times \text{H}_2\text{O}$	1.0393	1.0322	−0.0071	−13.855	−13.560	0.295	−0.085
t-LysH ⁺	1.0350	1.0280	−0.0071	n.a.	n.a.	n.a.	n.a.
$2\text{H}_2\text{O} \times \text{t-LysH}^+ \times \text{H}_2\text{O}$	1.0414	1.0335	−0.0079	−14.274	−13.964	0.310	−0.092
t-Lys12H1 ⁺ × t-Glu23O ^{−c}	1.0656	1.0552	−0.0104	−104.613	−104.058	0.555	
t-Glu23O [−] × t-Lys12H2 ^{++d}	1.0329	1.0260	−0.0068	−104.613	−104.609		0.004
t-Glu23O [−] × t-Lys12H3 ^{++d}	1.0292	1.0226	−0.0066	−104.613	−104.716		−0.104
$(2\text{H}_2\text{O}) \times \text{t-Lys12H}^+ \times \text{t-Glu23O}^{-e}$	1.0426	1.0358	−0.0068	−120.433	−120.225	0.207	
t-Glu23O [−] × t-Lys12H2 ⁺⁺ × $(2\text{H}_2\text{O})^e$	1.0735	1.0629	−0.0106	−33.391	−32.697	0.694	0.351
t-Glu23O [−] × t-Lys12H3 ⁺⁺ × $(2\text{H}_2\text{O})^e$	1.0365	1.0278	−0.0087	−10.226	−9.931	0.295	−0.077
t-Lys18H1 ⁺ × t-Glu64O ^{−d}	1.0350	1.0278	−0.0072	−60.846	−60.829	0.017	
t-Glu64O [−] × t-Lys18H2 ^{++d}	1.0349	1.0277	−0.0072	−60.846	−60.827		0.019
t-Glu64O [−] × t-Lys18H3 ^{++d}	1.0312	1.0241	−0.0071	−60.846	−60.917		−0.071
$(2\text{H}_2\text{O}) \times \text{t-Lys18H}^+ \times \text{t-Glu64O}^{-e}$	1.0304	1.0233	−0.0071	−58.822	−58.818	0.004	
t-Glu64O [−] × t-Lys18H2 ⁺⁺ × $(2\text{H}_2\text{O})^e$	1.0493	1.0406	−0.0087	−15.107	−14.707	0.400	0.035
t-Glu64O [−] × t-Lys18H3 ⁺⁺ × $(2\text{H}_2\text{O})^e$	1.0411	1.0327	−0.0084	−13.238	−12.941	0.297	−0.103
t-Lys39H1 ⁺ × t-Glu35O ^{−d}	1.1049	1.0924	−0.0125	−108.085	−106.969	1.116	
t-Glu35O [−] × t-Lys39H2 ^{++d}	1.0293	1.0225	−0.0068	−108.085	−108.222		−0.137
t-Glu35O [−] × t-Lys39H3 ^{++d}	1.0299	1.0232	−0.0067	−108.085	−108.200		−0.115
$(2\text{H}_2\text{O}) \times \text{t-Lys39H}^+ \times \text{t-Glu35O}^{-e}$	1.0624	1.0533	−0.0090	−118.765	−118.081	0.684	
t-Glu35O [−] × t-Lys39H2 ⁺⁺ × $(2\text{H}_2\text{O})^e$	1.0320	1.0245	−0.0075	−11.059	−10.816	0.243	−0.141
t-Glu35O [−] × t-Lys39H3 ⁺⁺ × $(2\text{H}_2\text{O})^e$	1.0345	1.0268	−0.0077	−24.223	−23.943	0.280	0.004
t-Lys58H1 ⁺ × t-Asp55O ^{−d}	1.1112	1.0987	−0.0125	−118.254	−117.072	1.182	
t-Asp55O [−] × t-Lys58H2 ^{++d}	1.0290	1.0222	−0.0068	−118.254	−118.406		−0.153
t-Asp55O [−] × t-Lys58H3 ^{++d}	1.0296	1.0230	−0.0066	−118.254	−118.379		−0.126
$(\text{H}_2\text{O}) \times \text{t-Lys58H}^+ \times \text{t-Asp55O}^{-e}$	1.0981	1.0862	−0.0118	−109.747	−108.662	1.085	
t-Asp55O [−] × t-Lys58H2 ⁺⁺ × $(\text{H}_2\text{O})^e$	1.0366	1.0289	−0.0077	−10.366	−10.115	0.251	−0.179
t-Asp55O [−] × t-Lys58H3 ⁺⁺ × $(\text{H}_2\text{O})^e$	1.0274	1.0207	−0.0067	−109.747	−110.027		−0.280
$(2\text{H}_2\text{O}) \times \text{t-Lys58H}^+ \times \text{t-Asp55O}^{-e}$	1.0582	1.0493	−0.0089	−128.880	−128.288	0.592	
t-Asp55O [−] × t-Lys58H2 ⁺⁺ × $(2\text{H}_2\text{O})^e$	1.0342	1.0269	−0.0073	−9.693	−9.430	0.263	−0.213
t-Asp55O [−] × t-Lys58H3 ⁺⁺ × $(2\text{H}_2\text{O})^e$	1.0611	1.0518	−0.0093	−34.319	−33.706	0.613	0.211
t-Lys57H1 ⁺ × t-PhosO ₄ ^{−d}	1.0732	1.0629	−0.0103	−555.662	−554.745	0.917	
t-PhosO ₄ [−] × t-Lys57H2 ^{++d}	1.0313	1.0245	−0.0068	−555.662	−555.480		0.181
t-PhosO ₄ [−] × t-Lys57H3 ^{++d}	1.0299	1.0231	−0.0068	−555.662	−555.544		0.118
$(2\text{H}_2\text{O}) \times \text{t-Lys57H}^+ \times \text{t-PhosO}_4^{-e}$	1.0543	1.0455	−0.0089	−566.091	−565.363	0.728	
t-PhosO ₄ [−] × t-Lys57H2 ⁺⁺ × $(2\text{H}_2\text{O})^e$	1.0361	1.0284	−0.0077	−8.108	−7.877	0.231	0.387
t-PhosO ₄ [−] × t-Lys57H3 ⁺⁺ × $(2\text{H}_2\text{O})^e$	1.0334	1.0261	−0.0073	−6.778	−6.484	0.294	0.200

^a t-Lys12, 18, 39, and 58 refer to protein G,²⁷ t-Lys57 to the HoxD9 homeodomain.³² ^b Primary isotope effect on interaction energies. ^c Secondary isotope effect on interaction energies. ^d H1 points toward the carboxylate, while H2 and H3 do not. ^e Hydrated t-lysine: H1 points toward the carboxylate while H2 and H3 points toward water. ^f No acceptor atom.

N–H distance, which parallels a decrease in heavy atom distance, showing that the salt bridge interaction becomes stronger. It can be seen in Figure 5 that the t-LysH⁺ and t-Lys18H⁺-carboxylate complexes have almost identical values for $^1\Delta^{15}\text{N}(\text{D})$ and N–H bond length, indicating no influence of counterion when present at a long distance. The value for a bare methylammonium ion is 0.63 ppm and can be considered corresponding to an infinite distance. Figure 5 provoke a question whether methylammonium molecule is a reliable model for lysine. It looks like substitution has a large effect, but this is because the symmetry is different in the ammonium ion and in the methylammonium ion. The symmetry is important in relation to how many NH bonds point toward the water and how many away and what the directions are. We have calculated the isotope effects on the

ethylammonium ion (by adding a methyl group to t-Lys39). For the non-hydrated case, we find a value of 0.57 ppm for the proton pointing toward the carboxylate group and 0.72 ppm for the protons present on the opposite side. For the hydrated case, we find a value of 0.63 ppm for the proton pointing toward the carboxylate group and 0.54 ppm and 0.58 ppm for the protons present on the opposite side. This indicates that substitution has no effect on the isotope effects (see Table 1). This also indicates that the methylammonium ion is a good model for lysines in the present context.

The present calculations could help to understand the variations in the $^1\Delta^{15}\text{N}(\text{D})$ of ammonium ions as a function of type and concentration.¹⁸ The larger magnitude observed for concentrated solutions of ammonium iodide and bromide compared

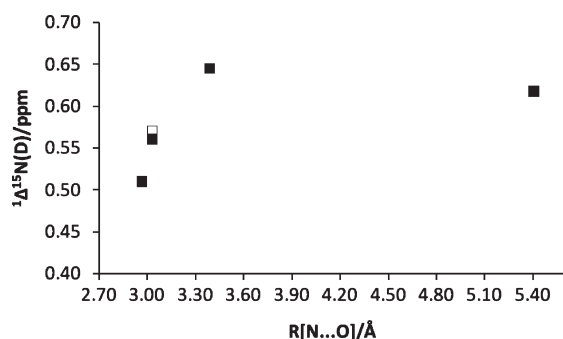


Figure 4. Plot of calculated ${}^1\Delta^{15}\text{N(D)}$ of non-hydrated t-Lys 12, 18, 39, 58 (■) and ethylammonium ion (□) for the proton pointed toward the carboxylate group vs $R[\text{N}\cdots\text{O}]$ (X-ray) distances.

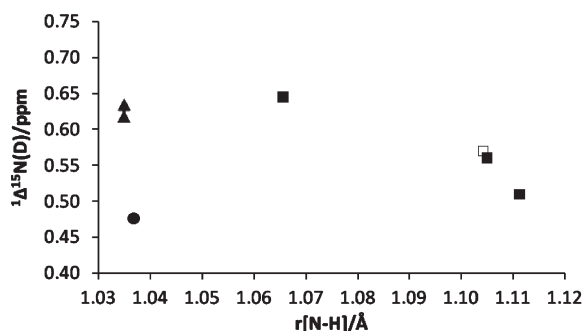


Figure 5. Calculated ${}^1\Delta^{15}\text{N(D)}$ of non-hydrated t-Lys 12, 39, 58 (■) and ethylammonium ion (□) for the proton pointing toward the truncated carboxylate group and non-hydrated t-Lys 18 and t-Lys (▲) and the ammonium ion (●) as a function of the calculated $r[\text{N-H}]$ distance.

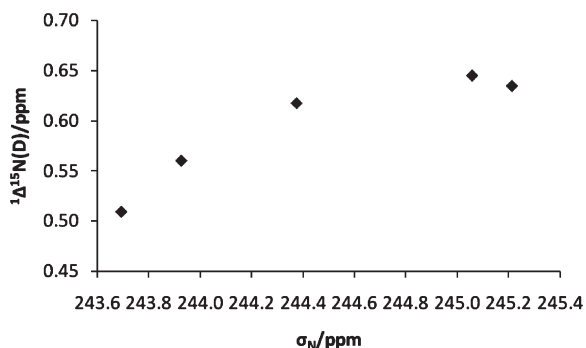


Figure 6. Plot of ${}^1\Delta^{15}\text{N(D)}$ of non-hydrated t-LysH⁺, t-Lys 12, 18, 39, 58 for the proton pointed toward truncated carboxylate group vs the calculated σ_{N} .

to very dilute solutions in water can be seen as an effect of the counterions squeezing out water from the first solvation shell.

It has previously been observed that one-bond isotope effects are proportional to shielding (chemical shift).¹² Figure 6 shows ${}^1\Delta^{15}\text{N(D)}$ versus the calculated isotropic nuclear shielding constants σ_{N} (direct H/D quantum treatment) of the methylammonium nitrogen atoms interacting with carboxylate oxygen atoms of different ionic complexes. A reasonable correlation is seen with a slope ${}^1\Delta^{15}\text{N(D)}/\sigma(\text{N})$ of approximately 0.078.

Effect of Water on Isotope Shifts. The addition of water leads to a lengthening of the N–H and N–D bonds (Table 2), the effect being significantly less for D than for H. This is the

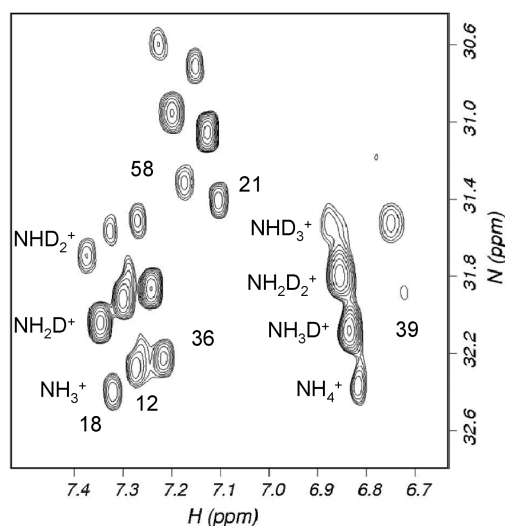


Figure 7. HISQC deuterium decoupled spectrum of the six lysine NH_3^+ groups of protein G B1 domain and ammonium ion at pH 4.47, 278 K in 40% D_2O .

expected result assuming that water forms weak hydrogen bonds, the effect being stronger for N–H. For an N–H or N–D in a salt bridge with a carboxylate, addition of water leads to a shortening of the N–H/D bond, the effect again being stronger for N–H. This is consistent with water weakening the salt bridge. The effect on ${}^1\Delta^{15}\text{N(D)}$ is dramatic (Table 1). In an unhydrated amine involved in a salt bridge, replacement of H by D for either of the two protons not in the salt bridge leads to a large increase in isotope shift. On hydration, these shifts become much smaller, and consequently addition of water consistently leads to a reduction in ${}^1\Delta^{15}\text{N(D)}$ (Table 1).

The effect of water on isotope shifts is of considerable interest because exposed salt bridges are very likely to be solvated, whereas buried salt bridges are more likely to be unsolvated. Therefore, the burial of salt bridges has a doubly important effect on the isotope shift. The effect is particularly clearly seen for lysine 58, for which we have carried out calculations with zero, two, and one water molecules (as observed in the crystal structure). Addition of water weakens the salt bridge and produces a larger value for ${}^1\Delta^{15}\text{N(D)}$ and shorter N–H bond length for the N–H proton pointing toward the carboxylate group, but a smaller value for ${}^1\Delta^{15}\text{N(D)}$ for the other two protons. Consequently, addition of water leads to a reduction in the averaged value for ${}^1\Delta^{15}\text{N(D)}$.

Experimental Measurements on Protein G B1 Domain.

Expression, purification, and sample preparation of protein G B1 domain was described in our previous work.¹⁰ The recording of nuclear magnetic resonance (NMR) experiments, data processing, and assignment of the six lysine NH_3^+ signals in 40% D_2O at pH 5.45, 4.95, 4.47, and 3.46 and temperature at 278 K for the protein G B1 domain were also described in the same work, but only the deuterium isotope effects on nitrogen and proton chemical shifts at pH 5.45 were described. Here, we present the experimental measured deuterium isotope effects on ${}^1\text{H}$ and ${}^{15}\text{N}$ chemical shifts induced by the substitution of deuterium at pH 4.47. At this pH, chemical exchange with solvent is slower, and hence experimental values can be determined for all six lysines, as well as ammonium ions, which are also present in the solution. An HISQC spectrum of the side chain lysine signals from the protein G B1 domain and ammonium ion is shown in Figure 7, and the experimental isotope effects are included in Table 1.

Three NH correlation peaks can be observed for each lysine, corresponding to NH_3^+ , NH_2D^+ , and NHD_2^+ groups (see labels on lysine 18). The HISQC spectrum also contains four ammonium ion signals, corresponding to NH_4^+ , NH_3D^+ , NH_2D_2^+ , and NHD_3^+ ions. All of these ions generate different signals for both ^{15}N and ^1H chemical shifts due to replacement of zero, one, or two protons by a deuteron with a consequent change in chemical shift as a result of the deuterium isotope effect. The relative abundance of these ions is given by the binomial distribution of the protons and deuterons. The HISQC spectrum contains a statistical distribution of protons and deuterons. The ratio of proton and deuteron isotopomers in the side chain lysine group, $\text{NH}_3^+:\text{NH}_2\text{D}^+:\text{NHD}_2^+$ and ammonium ion, $\text{NH}_4^+:\text{NH}_3\text{D}^+:\text{NH}_2\text{D}_2^+:\text{NHD}_3^+$ is approximated to be 0.22:0.43:0.29 and 0.13:0.34:0.34:0.15, respectively, which matches well to the experimental ratios. Our interest is restricted to study the averaged size of this effect per deuteron: within experimental error, deuterium isotope effects are identical for each deuteron added.^{10,14}

For protein G, X-ray structures²⁷ suggest that lysine 12, 39, and 58 are likely to be involved in salt bridges exposed on the surface of the protein, while lysine 36 could possibly also be involved in a salt bridge. The experimentally observed $^1\Delta^{15}\text{N}(\text{D})$ isotope effects for the lysines obtained by subtraction of the $\text{N}(\text{D})$ chemical shift from that of the $\text{N}(\text{H})$ chemical shift for each species are seen to be very similar (Table 1). In addition, the chemical shifts for the lysine N^ξ are also very similar, with a variation of less than 0.7 ppm.¹⁰ This is consistent with the expected correlation between $^1\Delta^{15}\text{N}(\text{D})$ and ^{15}N shift (Figure 6).¹² For $^2\Delta^1\text{H}(\text{D})$ the values are clearly negative and close to -0.027 ppm (Table 1) except for ammonium ions for which the value is only -0.018 ppm which is very close to the value (-0.017 ppm) obtained by Hansen and Lycka.¹²

It is clear that the calculated $^1\Delta^{15}\text{N}(\text{D})$ isotope effects are larger than those found in solution. The influence of water is a determining factor, and the $\text{N}\cdots\text{O}$ distance between the lysine nitrogen and the water oxygen would only have to be decreased slightly to obtain calculated values in agreement with observation. However, the solution study concluded that the salt bridges found in the crystal are of very limited stability in water. Our results are consistent with this conclusion, suggesting a major weakening of the salt bridge produced by solvation.

Interestingly, a very similar $^1\Delta^{15}\text{N}(\text{D})$ value of 0.35 ppm can be extracted from the results of Iwahara et al.³² for lysine 57 of HoxD9 homeodomain bound to DNA. The authors assume that the lysine is forming a buried salt bridge with the oxygen atom of a phosphate group with a $\text{N}\cdots\text{O}$ distance less than 3.2 Å. In Tables 1 and 2, data for a truncated lysine modeling for this system are included. As seen from Table 1, the calculated isotope effect using only a phosphate counterion is 0.63 ppm, whereas adding water decreases the value to 0.49 ppm, a difference in calculated versus observed similar to what is found for ammonium ions (see above). This suggests that solvation is also occurring for lysine 57 in the homeodomain, the effect being greater than that modeled here. Thus, even though the salt bridge is buried in the protein/DNA interface, it is still very significantly weakened by solvation.

CONCLUDING REMARKS

This paper describes the calculation of deuterium isotope effects on chemical shifts using a MC_MO-HF method based on a non-Born–Oppenheimer approximation for the direct

treatment of the H/D nuclear quantum effect. This method combined with calculations of nuclear shielding is a fast method as compared to previous calculations of changes in bond distances upon deuteration based on potential wells and a better method compared to just guessing this change. Using the above theoretical method, we observed a smaller value of $^1\Delta^{15}\text{N}(\text{D})$ for a shorter $\text{N}\cdots\text{O}$ distance that is closely related to the ^{15}N shielding. For the liquid state, inclusion of inner shell solvation could easily be implemented. It was shown that using distances obtained from the crystal structure did not lead to values close to the experimental ones, most likely as shown earlier,^{10,32} because the salt bridges are almost non-existent in solution.

AUTHOR INFORMATION

Corresponding Author

*Saif Ullah, Department of Science, Systems and Models, Roskilde University, P.O. Box 260, DK-4000 Roskilde, Denmark. E-mail: sullah@ruc.dk, tel.: +45 4674 2327, fax: +45 4674 3011.

REFERENCES

- (1) Scheiner, S. *Hydrogen Bonding. A Theoretical Perspective*; Oxford University Press: New York, 1997.
- (2) Smith, D. A. *Modeling the Hydrogen Bond*; American Chemical Society: Washington, DC, 1994; Vol. 569.
- (3) Kim, J.; Mao, J.; Gunner, M. R. *J. Mol. Biol.* **2005**, *348*, 1283–1298.
- (4) Dong, F.; Zhou, H. X. *Biophys. J.* **2002**, *83*, 1341–1347.
- (5) Takano, K.; Tsuchimori, K.; Yamagata, Y.; Yutani, K. *Biochemistry* **2000**, *39*, 12375–12381.
- (6) Vijayakumar, M.; Zhou, H. X. *J. Phys. Chem. B* **2001**, *105*, 7334–7340.
- (7) Phelan, P.; Gorfe, A. A.; Jelesarov, I.; Marti, D. N.; Warwicker, J.; Bosshard, H. R. *Biochemistry* **2002**, *41*, 2998–3008.
- (8) Sali, D.; Bycroft, M.; Fersht, A. R. *J. Mol. Biol.* **1991**, *220*, 779–788.
- (9) Strop, P.; Mayo, S. L. *Biochemistry* **2000**, *39*, 1251–1255.
- (10) Tomlinson, J. H.; Ullah, S.; Hansen, P. E.; Williamson, M. P. *J. Am. Chem. Soc.* **2009**, *131*, 4674–4684.
- (11) Munch, M.; Hansen, A. E.; Hansen, P. E.; Bouman, T. D. *Acta Chem. Scand.* **1992**, *46*, 1065–1071.
- (12) Hansen, P. E.; Lycka, A. *Acta Chem. Scand.* **1989**, *43*, 222–232.
- (13) Lycka, A.; Hansen, P. E. *Magn. Reson. Chem.* **1985**, *23*, 973–976.
- (14) Sanders, J. K. M.; Hunter, B. K.; Jameson, C. J.; Romeo, G. *Chem. Phys. Lett.* **1988**, *143*, 471–476.
- (15) Hansen, P. E.; Hansen, A. E.; Lycka, A.; Buvaribarcza, A. *Acta Chem. Scand.* **1993**, *47*, 777–788.
- (16) Perrin, C. L.; Gipe, R. K. *J. Am. Chem. Soc.* **1986**, *108*, 1088–1089.
- (17) Jameson, C. J. *Isotopes in the Physical and Biomedical Sciences Isotopic Application in NMR Studies*; Buncel, E., Jones, J. R., Eds.; Elsevier Science: Amsterdam, The Netherlands, 1991; Vol. 2.
- (18) Abildgaard, J.; Bolvig, S.; Hansen, P. E. *J. Am. Chem. Soc.* **1998**, *120*, 9063–9069.
- (19) Benedict, H.; Limbach, H. H.; Wehlan, M.; Fehllhammer, W. P.; Golubev, N. S.; Janoschek, R. *J. Am. Chem. Soc.* **1998**, *120*, 2939–2950.
- (20) Vener, M. V. *Chem. Phys.* **1992**, *166*, 311–316.
- (21) Tachikawa, M. *Chem. Phys. Lett.* **2002**, *360*, 494–500.
- (22) Ishimoto, T.; Tachikawa, M.; Nagashima, U. *Int. J. Quantum Chem.* **2009**, *109*, 2677–2694.
- (23) Wong, K.-Y.; Richard, J. P.; Gao, J. *J. Am. Chem. Soc.* **2009**, *131*, 13963–13971.
- (24) Wong, K.-Y.; Gao, J. *J. Chem. Theory Comput.* **2008**, *4*, 1409–1422.
- (25) Ishimoto, T.; Tachikawa, M.; Nagashima, U. *J. Chem. Phys.* **2006**, *125*.

- (26) Kikuta, Y.; Ishimoto, T.; Nagashima, U. *Chem. Phys.* **2008**, *354*, 218–224.
- (27) Gallagher, T.; Alexander, P.; Bryan, P.; Gilliland, G. L. *Biochemistry* **1994**, *33*, 4721–4729.
- (28) Ditchfield, R. *Mol. Phys.* **1974**, *27*, 789–807.
- (29) Wolinski, K.; Hinton, J. F.; Pulay, P. *J. Am. Chem. Soc.* **1990**, *112*, 8251–8260.
- (30) Frisch, M. J.; Trucks, G. W.; Schlegel, H. B.; Scuseria, G. E.; Robb, M. A.; Cheeseman, J. R.; Montgomery, J. A.; Vreven, T.; Kudin, K. N.; Burant, J. C.; Millam, J. M.; Iyengar, S. S.; Tomasi, J.; Barone, V.; Mennucci, B.; Cossi, M.; Scalmani, G.; Rega, N.; Petersson, G. A.; Nakatsuji, H.; Hada, M.; Ehara, M.; Toyota, K.; Fukuda, R.; Hasegawa, J.; Ishida, M.; Nakajima, T.; Honda, Y.; Kitao, O.; Nakai, H.; Klene, M.; Li, X.; Knox, J. E.; Hratchian, H. P.; Cross, J. B.; Bakken, V.; Adamo, C.; Jaramillo, J.; Gomperts, R.; Stratmann, R. E.; Yazyev, O.; Austin, A. J.; Cammi, R.; Pomelli, C.; Ochterski, J. W.; Ayala, P. Y.; Morokuma, K.; Voth, G. A.; Salvador, P.; Dannenberg, J. J.; Zakrzewski, V. G.; Dapprich, S.; Daniels, A. D.; Strain, M. C.; Farkas, O.; Malick, D. K.; Rabuck, A. D.; Raghavachari, K.; Foresman, J. B.; Ortiz, J. V.; Cui, Q.; Baboul, A. G.; Clifford, S.; Cioslowski, J.; Stefanov, B. B.; Liu, G.; Liashenko, A.; Piskorz, P.; Komaromi, I.; Martin, R. L.; Fox, D. J.; Keith, T.; Laham, A.; Peng, C. Y.; Nanayakkara, A.; Challacombe, M.; Gill, P. M. W.; Johnson, B.; Chen, W.; Wong, M. W.; Gonzalez, C.; Pople, J. A. *Gaussian 03, Revision C.02*; Gaussian Inc.: Wallingford, CT, 2004.
- (31) Dos, A.; Schimming, V.; Tosoni, S.; Limbach, H.-H. *J. Phys. Chem. B* **2008**, *112*, 15604–15615.
- (32) Iwahara, J.; Jung, Y. S.; Clore, G. M. *J. Am. Chem. Soc.* **2007**, *129*, 2971–2980.